

## Multisystemic Pediatric Langerhans cell histiocytosis: a comprehensive clinico-pathological and BRAF V600E mutation study at autopsy

Gargi Kapatia<sup>a</sup> , Prateek Bhatia<sup>b</sup> , Minu Singh<sup>b</sup> , Richa Jain<sup>b</sup> ,  
Deepak Bansal<sup>b</sup> , Kirti Gupta<sup>a</sup> 

**How to cite:** Kapatia G, Bhatia P, Singh M, Jain R, Bansal D, Gupta K. Multisystemic Pediatric Langerhans cell histiocytosis: a comprehensive clinico-pathological and BRAF V600E mutation study at autopsy. *Autops Case Rep* [Internet]. 2020 Apr-Jun;10(2):e2020154. <https://doi.org/10.4322/acr.2020.154>

### ABSTRACT

Langerhans cell histiocytosis (LCH), a disorder of antigen-presenting cells, is the commonest disorder of the mononuclear phagocytic system. Diagnosis is always challenging due to heterogeneous clinical presentation. However, with the evolution and better understanding of its biology, many of these children are being diagnosed early and offered appropriate therapy. Despite these advances, in developing countries, an early diagnosis is still challenging due to resource constraints for specialized tests. As a result, many patients succumb to their disease. Autopsy data on LCH is notably lacking in the literature. We sought to analyze the clinical (including mutational) and morphologic features at autopsy in six proven cases of LCH. This study includes a detailed clinico-pathological and mutational analysis of 6 proven cases of LCH. Presence of BRAF V600E mutation was assessed by both Real Time PCR and Sanger sequencing. A varied spectrum of organ involvement was noted with some rare and novel morphological findings, like nodular bronchiolocentric infiltration of LCH cells, lymphovascular emboli of LCH cells, and paucity of eosinophils within the infiltrate; these features have not been described earlier. Surprisingly, all cases were negative for BRAF V600E mutation on both RQ-PCR and Sanger sequencing. The present study is perhaps the first autopsy series on LCH. This extensive autopsy analysis represents a correlation of pathological features with clinical symptoms which provides clues for a timely diagnosis and appropriate therapeutic intervention. Also, our findings hint at the low frequency of BRAF V600E mutation in our LCH patients.

### Keywords

Autopsy; Histiocytosis, Langerhans-Cell; Mitogen-Activated Protein Kinase Kinases; Proto-Oncogene Proteins B-raf

### INTRODUCTION

Langerhans cell histiocytosis (LCH) is a rare histiocytic disorder characterized by the infiltration of tissues with a distinct dendritic cell, the Langerhans cell (LC). It is the commonest of all histiocytic disorders. This LC is distinguished from other dendritic cells by their peculiar morphological, immunohistochemical and ultrastructural features which include the presence of

intracellular Birbeck granules and surface expression of S100, CD1a and CD207 (Langerin).<sup>1</sup> The clinical presentation ranges from relatively benign self-limited disease to a devastating multisystem disease, latter having poor prognosis.<sup>2</sup> The severity of LCH is usually age-related. Extensive disseminated multisystem variants with a poor prognosis and mortality rate

<sup>a</sup> Post Graduate Institute of Medical Education & Research (PGIMER), Department of Histopathology. Chandigarh, India.

<sup>b</sup> Post Graduate Institute of Medical Education & Research (PGIMER), Department of Pediatrics. Chandigarh, India.



up to 50%<sup>3</sup> have been primarily described in early childhood. In contrast, multifocal single-system disease is often diagnosed in children aged up to 5 years. Unifocal bone restricted disease primarily hits older children.<sup>4</sup> The presenting symptoms depend upon the system involved and are wide-ranging from cutaneous symptoms, ear discharge, bone pain, fever, and lymphadenopathy. Recently, the identification of MAP kinase pathway alterations, particularly BRAF V600E mutation in LCH, has settled the earlier debate on its inflammatory versus clonal/neoplastic etiology. BRAF V600E mutation has been identified in up to 50% of cases of pediatric LCH and 35% of adult cases.<sup>5,6</sup> Although BRAF V600E mutation in LCH does not correlate with clinical severity or classification, the presence of this mutation has implications both for molecular diagnosis and for targeted therapy with BRAF kinase inhibitors such as Vemurafenib. Additionally, it is useful for monitoring treatment efficacy and has been observed to indicate an increased risk of recurrence compared to those without the mutation.<sup>7,8</sup>

The main purpose of the study is to emphasize the different histological patterns of organ infiltration in LCH at autopsy and to evaluate the presence of BRAF V600E mutation in fatal cases of LCH. Autopsy data on LCH notably lacks in the literature with histopathological evaluation being limited to rare case reports (including two cases which are part of this data).<sup>9,10</sup> Also, BRAF mutational status so far has been assessed in small case series.<sup>5,6,8,11,12</sup> To the best of our knowledge, this is the first autopsy study on LCH providing a detailed analysis of clinic-pathological findings and illustrating the unusual locations and pattern of infiltration. Our third objective of correlating the organ infiltration with mutational status could not be fulfilled as all the cases were negative for BRAF V600E mutation. Nonetheless, analysis of autopsy data helps in better understanding the clinical manifestations and provides clues for timely intervention, which might contribute to improving the morbidity and mortality in these patients.

## **MATERIALS AND METHODS**

The study included a detailed clinico-pathological analysis of 6 autopsy cases of LCH performed at our Institute over the past 10 years. The clinical data and records were retrieved from case records and files of the

pediatric clinics, and the autopsies were performed in the Department of Histopathology. The study was approved by Departments' review boards as per the existing practice at our Institute. Written, informed consent was taken for the autopsy. The clinical data included age at presentation and diagnosis, presenting complaints, and detailed laboratory investigations. Family history and birth history was analyzed wherever provided. In four cases, all organs excluding the brain were examined, while in one case brain was also autopsied along with the rest of the organs. For each autopsy, detailed gross and microscopic examination of both lungs with the tracheobronchial tree, heart, liver, spleen, pancreas, kidneys, gastrointestinal tract, bone marrow, lymph nodes, skin, testis, skeletal muscle, and adrenals was performed. Special histochemical stains, such as Ziehl Neelsen (ZN), Gram, Periodic acid-Schiff (PAS), and Grocott's stain were used to identify superadded bacterial and fungal infections. Immunostain for CD1a, S100, CD68 and/or Langerin were performed in all the cases to confirm the diagnosis. Electron microscopic examination was done in two cases.

## **Mutational Analysis**

Mutation analysis was performed in all six cases by both Real-time PCR (RQ-PCR) and Sanger sequencing. Briefly, FFPE blocks or autopsy tissue sections with tumor involvement and presence of at least > 30% tumor volume were selected for downstream analysis. Blocks were further macro-dissected to avoid contamination from surrounding normal tissue. DNA was extracted using the QIAmp DNA FFPE extraction kit (Qiagen, Germany) as per manufacturer's instructions. DNA quality check based on electrophoretic gel assessment of bands and nanoquant ratio was performed before further PCR analysis. RQ-PCR was carried out using Taq-Man probes (Applied Biosystems) according to the manufacturer's protocol, utilizing Applied Biosystem's StepOnePlus RQ-PCR system. The data was analyzed using Applied Biosystem's Mutation Detector Software. BRAF mutation was further confirmed by Sanger sequencing on the ABI 3730 Genetic Analyzer using forward primer TGCTTGCTCTGATAGGAAAATG and reverse primer CCACAAAATGGATCCAGACA. Following PCR conditions were used- denaturation-95°C (30 sec), annealing-57°C (30 sec) and extension-72°C (30 sec) for 35 cycle Mutation analysis was performed in all six cases by Sanger sequencing.

## RESULTS

### Clinical Characteristics and Investigations

Six patients (all males) with final autopsy diagnosis of LCH were included in the study. Out of 6 cases, three cases had a clinical diagnosis of LCH. The clinical details and investigations are summarized in Table 1.

### Autopsy Findings

The detailed autopsy findings are summarized in Table 2. There were six cases diagnosed as multisystemic LCH on autopsy. All cases were males with a mean age of 1.8 years (10 months-3.5 years). Pleural effusion was noted in 4 cases, ascites in 3 cases and pericardial effusion in 1 case.

### Frequency of Organ Infiltration (Figure 1)

The classical Langerhans cells demonstrated convoluted nuclei with vesicular chromatin, nuclear grooves, and characteristic Birbeck granules within the cytoplasm on electron microscopy performed from the paraffin-embedded tissue in two cases. LCs in all cases were immunoreactive for CD1a, S100, and CD68 (Figures 2A to 2D).

The lymph node and the liver were the two organs that were universally involved by LCH cells in all the cases ( $n=6$ , 100%). Lungs and spleen involvement were the second commonest in frequency ( $n=5$ , 83.3%). The pancreas was involved in 4 of the cases (66.7%) followed by gastrointestinal tract (GIT) and bone marrow in 3 cases (50%). Kidney, skin and, thymus were infiltrated in 2 subjects each (33.3%). Rare organs to be infiltrated included the heart (case#2), testes (case#6), thymus

(case#1), and choroid plexus (case#6) in one case each (16.7%). Hepatosplenomegaly was noted in 5 subjects (83.3%).

### Pattern of Infiltration by LC (Table 2):

#### *Liver (n=6/6)*

This was seen both in the sinusoids and in portal tracts. It was not accompanied by eosinophils or giant cells. A single case showed injury to bile duct with fibrosis and destruction with infiltrate showing admixture of eosinophils (Figure 3A-C).

#### *Lymph Node (n=6/6)*

There was both total and subtotal effacement of nodal architecture by the infiltrate. In a single case, the infiltrate was predominately seen filling up the sinuses and subcapsular regions. Giant cells, neutrophils, and plasma cells were not seen. No accompanying necrosis or fibrosis was noted. Two cases (case#1 and #2) showed lymphovascular emboli of LC within the subpleural vessels and those around lymph nodes (Figures 4A-C).

#### *Lungs (n=5/6)*

In 3 cases, the pleura showed a thick plaque-like infiltrate that microscopically showed large subpleural deposits of LC, admixed with a variable number of lymphocytes and eosinophils. The lung infiltrate was dominantly seen along the peribronchiolar interstitium and alveolar interstitium. In two cases, nodular collections of LCs were seen filling up the alveolar lumen while in the other two cases, the infiltrate was seen in the form of granulomas (Figures 5A-D). Cytomegalovirus inclusions (CMV) were noted within the lymph nodes ( $n=2/6$ ) and lungs ( $n=1/6$ ) (Figure 5D).

#### *Spleen (n=5/6)*

The infiltrate was mostly seen within the red pulp (Figure 6). Granulomas were seen in a single case.

#### *Heart (n=1/6)*

Infiltration of heart was very unusual. In one case, large nodular deposits on the pericardial surface distorted the shape of the heart. There was transmural infiltration of the ventricular wall by LC with bi-ventricular hypertrophy (Figures 7A-C). The heart valves were, however, normal in this case.

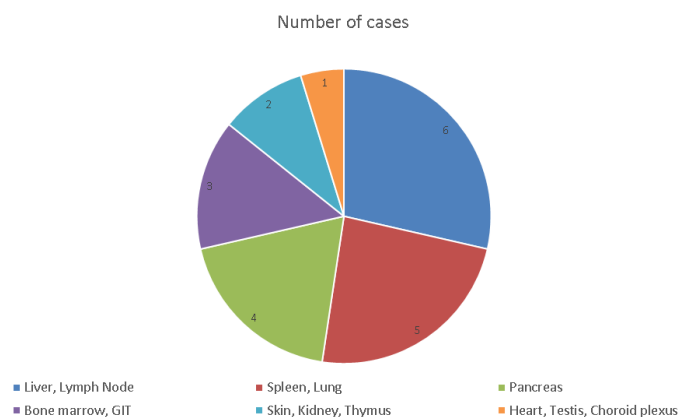


**Figure 1.** Pie chart depicting the frequency of organ infiltration.

**Table 1.** Relevant clinical details and investigations in LCH cases.

#	Age Gender	Clinical Symptoms	Family/Birth History	Clinical diagnosis	Microbiology	Radiological work up	Antemortem biopsy	Autopsy Diagnosis
1	1.5yrs/M	Rash, bilateral ear discharge, Fever, pallor, abdominal distension Swelling of gums and neck	1 <sup>st</sup> child (male) expired at birth of unknown cause, Index child was the 2 <sup>nd</sup> sibling	Multi-systemic LCH, sepsis pulmonary hemorrhage	Blood -Sterile; Urine - Sterile; Mantoux: Non-reactive;	Multiple lytic lesions head and face bones. Multiple enlarged conglomerated submandibular lymph nodes. HSM with ascites. Ill-defined GGOs with interstitial thickening in both lungs, small nodules in LLL and RLL; pleural effusion.	Hypercellular bone marrow with increased histiocytes and hemophagocytosis Skin biopsy: Suggestive of LCH.	Multisystemic LCH with early bronchopneumonia and alveolar hemorrhage
2	3.5yrs/M	Fever, Cough and respiratory distress	Previous 2 sibling deaths (at 3yrs and 9 months). He was the 4 <sup>th</sup>	Multidrug resistant TB	Blood and Urine: Sterile	HSM, mediastinal lymphadenopathy. Heterogeneous pulmonary opacities, multiple, bilateral pulmonary nodules with central cavitation.	lung biopsy misinterpreted as epithelioid granuloma	Multisystemic LCH with pneumonia
3	1.5yrs/M	swelling of the neck	insignificant	Multi-systemic LCH	Blood culture: Sterile	Lytic skull lesions	lymph node FNAC presumptive Bone marrow LCI	Multisystemic LCH with pneumonia
4	3yrs/M	swelling of left thigh after trauma; seborrheic dermatitis; and papules over nape of neck and back Fever Ear discharge	Gravida one ended in first trimester spontaneous abortion. Immunized for age.	Relapsing refractory multisystemic LCH with Febrile neutropenia and Pulmonary bleed	Blood culture: Sterile Ear discharge- Acinetobacter spp	Pathological fracture shaft of femur Expansile lytic space occupying lesion- Left femoral neck, Distal trochanter and Proximal shaft	Skin Biopsy- LCH Bone marrow- infiltration by LCH	Multisystemic LCH with pneumonia pulmonary hemorrhage, DAD, Candida ulcer in esophagus
5	10 m/M	Abdominal, distension, Fever, Altered sensorium, Rapid breathing	2nd in birth order, elder sibling healthy.	refractory septic shock, coagulopathy, pulmonary hemorrhage.	Blood culture: Sterile Urine culture: Sterile	HSM with bilateral increased renal cortical Medastinal widening by Lymph node mass encasing the vessels	Not done	Multisystemic LCH with confluent necrotizing pneumonia, pulmonary hemorrhage and DAD
6	1yr/M	Fever, pallor and lethargy, abdominal distension jaundice	Insignificant.	Hemo phagocytic lymphohistiocytosis (HLH), Pulmonary hemorrhage	Blood culture: S. aureus (MSSA)	HSM	Marrow: Megaloblastic erythroid hyperplasia with dyserythropoiesis, Large cells with great amount of cytoplasm, hemophagocytosis, iron overload Skin: hyperkeratosis thin epidermis. Dermis with mild lymphomononuclear infiltrates.	Multisystem LCH with reactive hemophagocytosis, secondary hemosiderosis and EMH in liver and spleen

DAD= diffuse alveolar damage; EMH= Extramedullary hematopoiesis; GGO= ground glass opacity; HSM= Hepatosplenomegaly; LCI= Langerhans cell Infiltration; LCH= Langerhans cell histiocytosis.; LUL= Left lower lobe; M= Male; MSSA= Methicillin-sensitive Staphylococcus aureus; RLL= Right lower lobe; TB= Tuberculosis; yrs= Years; # Serial Number.

**Table 2.** Summary of the autopsy findings in the 6 cases (numbering of cases is the same of Table 1).

#	Skin	Lymph node	Spleen	Liver	Lungs	Bone Mar- row	Kidneys	GIT	Pancreas	Others
1.	LCi	large amount of LC filling up the sinuses and subcapsular regions.	Enlarged. Extensive red pulp. LCi Foci of EMH and hemo phagocytosis	Enlarged. LC within the sinusoids and portal triaditis Foci of EMH and hemo phagocytosis	LCH infiltrate pneumonia; Alveolar hemorrhage. granulomas; few eosinophils. Prominent arterioles	Normocellular clusters of LCi within the paratrabecular spaces.	Focal LCi in the kidneys	LCi	Focal LCi	Thymus: LCi, microscopic cysts. Heart: Extensive LCi of both ventricles with bi-ventricular hypertrophy.
2	NAD	Enlarged. LCi	Enlarged. LCi	Enlarged. LCi	Bronchiolocentric nodular LCi; pneumonia, Occasional eosinophils, Grade II PAH, granulomas present ( <i>M.tuberculosis</i> negative)	Occasional LCi	NAD	NAD	LCi, inter- and intra-acinar fibrosis and inflammation	Heart: LCi
3	NAD	Enlarged. LCi	NAD	Enlarged. LCi. Many eosinophils. Injury to periductal bile ducts.	Pneumonia	NAD	Focal LCi in the kidneys	NAD	LCi along with localized acinar destruction	-
4	LCi	paracortical expansion due to LCi along with eosinophils.	Enlarged. LCi	Enlarged. LCi	LCi Pneumonia; hemorrhage, DAD and candida abscess. LCi confluent necrotizing pneumonia, hemorrhage and DAD	LCi	NAD	LCi	Normal	Thymus- LCi
5	NAD	Enlarged. LCi	Enlarged. LCi	Enlarged. LCi	LCi confluent necrotizing pneumonia, hemorrhage and DAD	NAD	NAD	NAD	LCi	NAD
6	NAD	Enlarged. LCi	Enlarged. LCi Hemosiderosis	Enlarged. LCi. Hemosiderosis	LCi	NAD	NAD	LCi	Normal	Testis and choroid plexus: LCi

DAD= Diffuse alveolar damage; EMH= Extramedullary hemophagocytosis; LCi = Langerhans cell infiltration; NAD= no abnormality detected; PAH= Pulmonary arterial hypertension; # Serial Number.

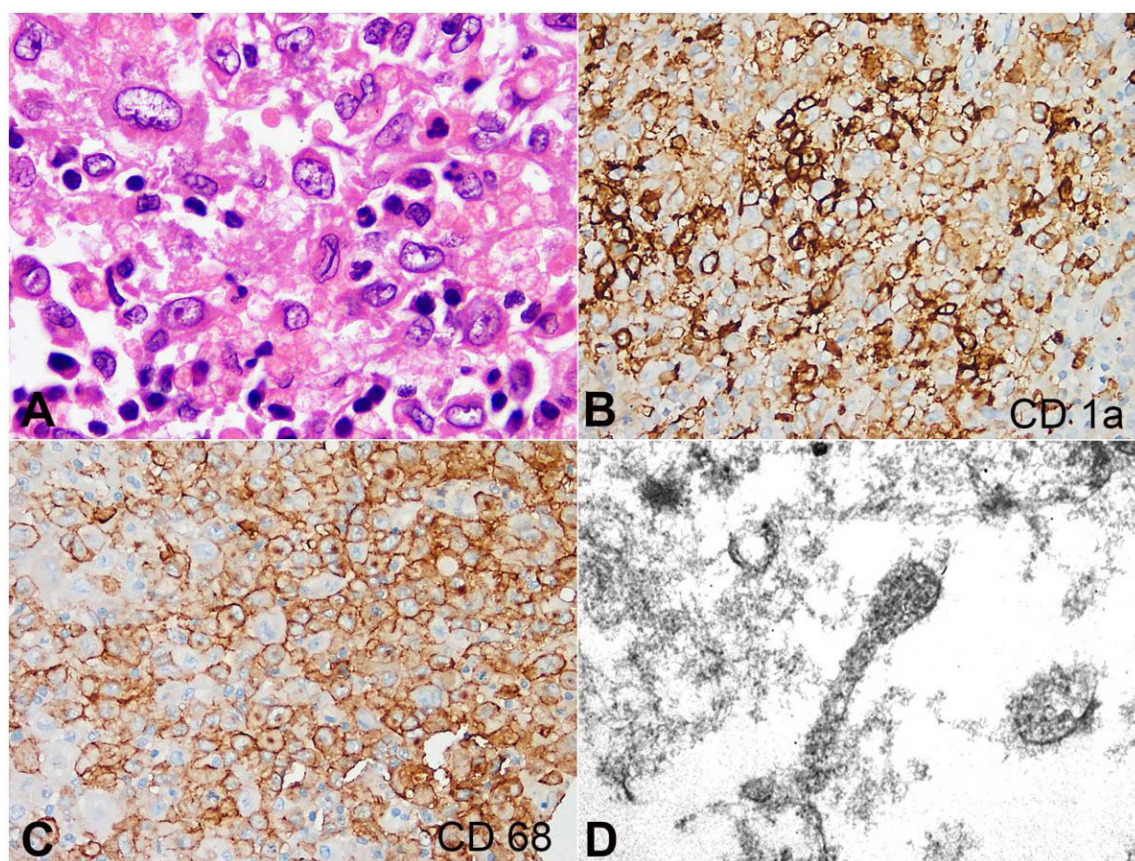


**Figure 2.** Photomicrographs of the lymph node showing in **A** – Characteristic Langerhans cells with convoluted nuclei and nuclear grooves (H&E x1000); **B, C** – Langerhans cells immunoreactive for CD1a and CD68 (**B** and **C** x400); **D** – Racket-shaped Birbeck granules within the cytoplasm of LC (uranyl acetate with lead citrate, x36,000).

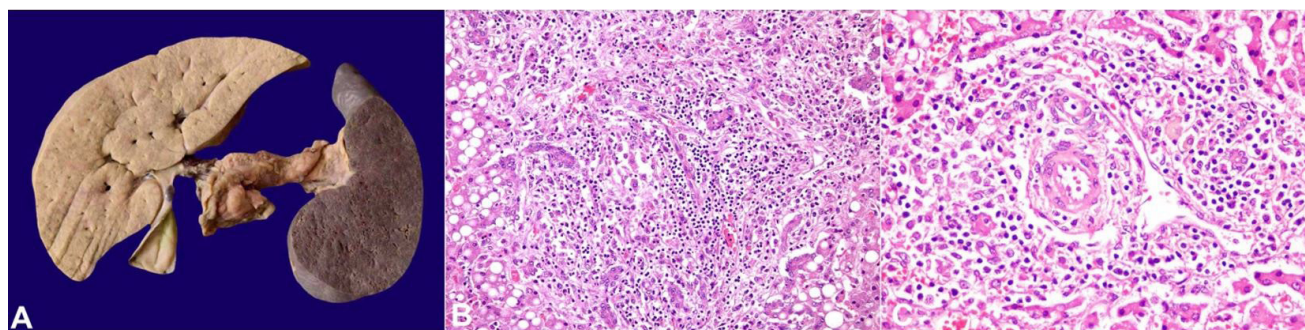


**Figure 3.** **A** – Gross view of the enlarged liver and spleen. **B, and C** – Photomicrographs of the liver. **B** - Cellular infiltrate within the portal tracts, and extending to the periportal areas (H&E x200); **C** – LC within the portal tracts causing destruction of bile ducts (H&E x400).

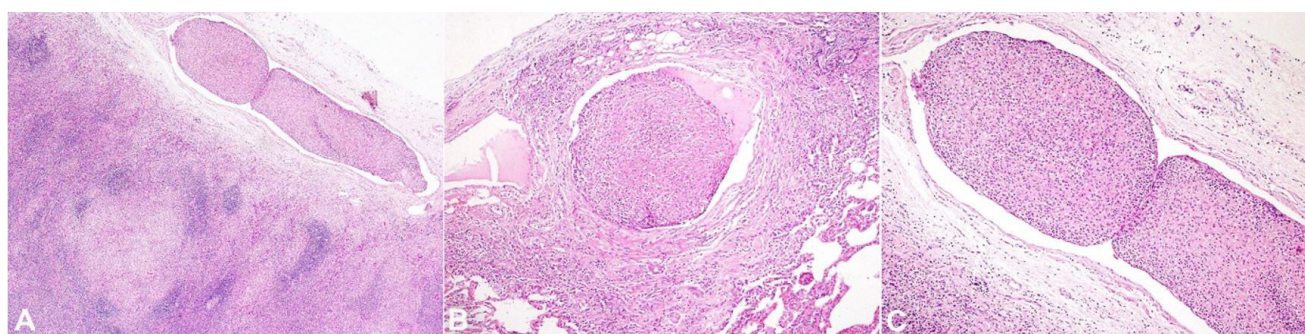


**Figure 4.** Photomicrographs of the lymph node. **A, B** – Lymphovascular emboli comprising of LC and accompanying cells enmeshed within fibrin (x100, B x200 respectively); **C** – High magnification showing the lymphovascular emboli comprising of LC (H&E x400).

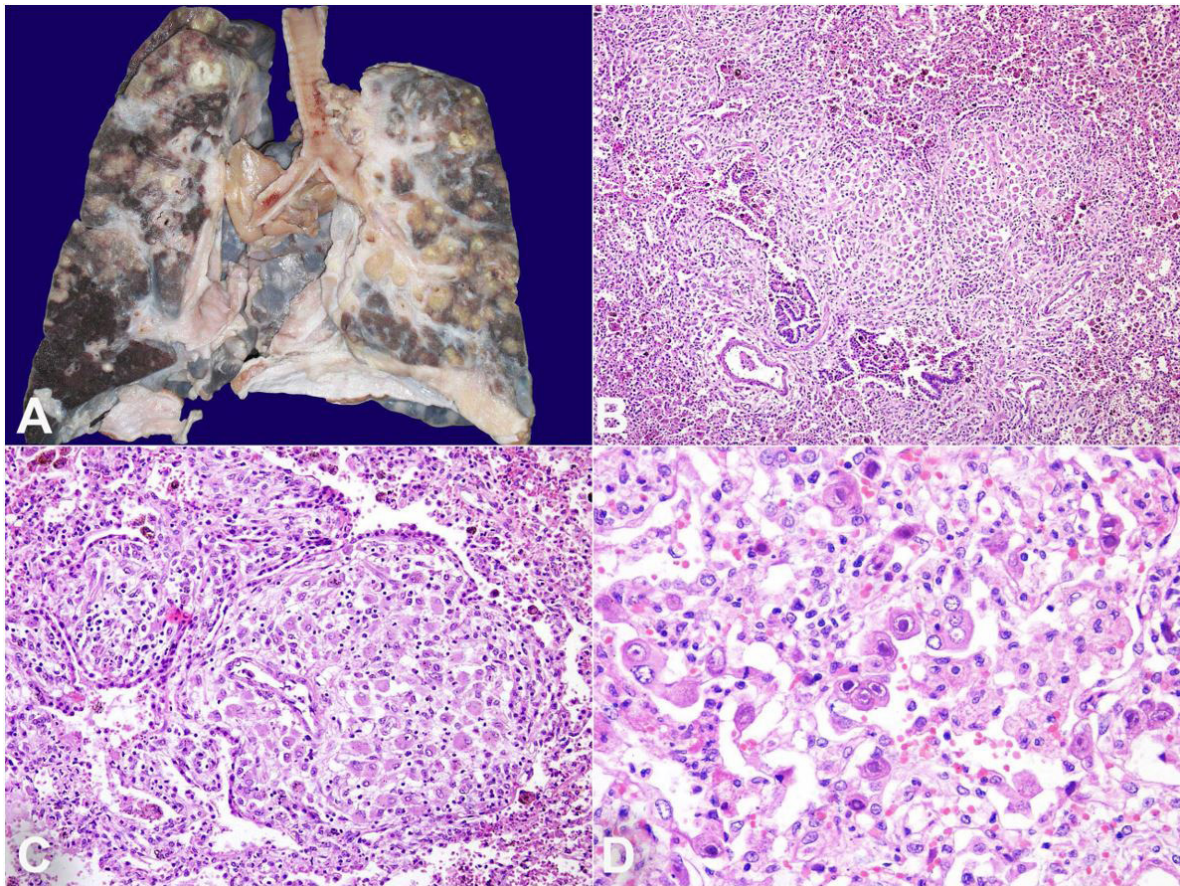


**Figure 5.** **A** – Gross view of the cut surface of both lungs showing nodules centered on the airways; **B** – Bronchiolocentric infiltrate seen within the lung parenchyma (H&E x200); **C** – LC infiltration causing destruction of the airways (H&E x400); **D** – Cytomegalovirus inclusions (CMV) seen lining the alveolar epithelial cells (H&E x400).

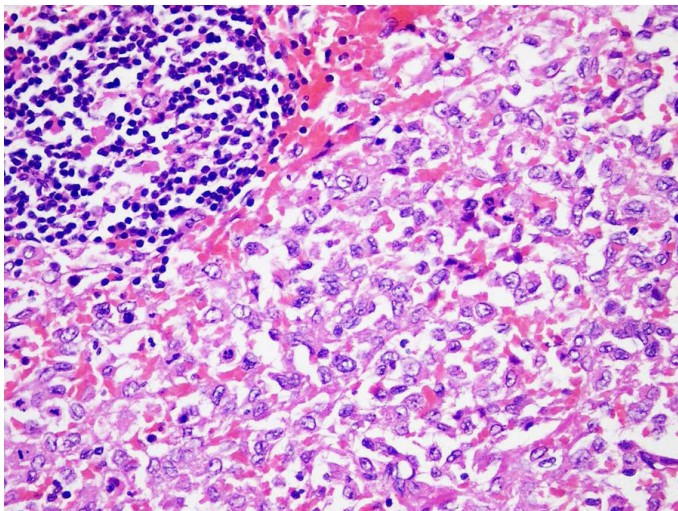


**Figure 6.** Photomicrograph of the spleen showing a subtotal effacement of nodal architecture by LC and accompanying cells (H&E x200).

#### *Gastrointestinal Tract (n=3/6)*

Infiltration of the intestine was seen in three cases wherein the lamina propria was expanded by a diffuse

infiltrate without any ulceration of the overlying mucosa. In contrast, in a single case, the overlying mucosa showed multiple punched out hemorrhagic ulcers (Figures 8A and 8B).

#### *Kidneys (n=2/6)*

Infiltrate was noted within the interstitium.

Unusual sites for infiltration included pancreas (n=4/6) (Figure 8C), heart (n=1/6), GIT in three and testis, thymus (Figure 8D), and choroid plexus in a single case each.

#### *Other Associated Findings*

Bronchopneumonia was seen in 5 subjects (83.3%), which was bacterial in all cases. Pulmonary hemorrhage was seen in 3 cases (50%), and diffuse alveolar damage was noted in 2 cases (33.3%). One of the cases (case#2) showed ill-formed LCH granulomas mimicking tuberculosis, both clinically and histologically (Figures 9A-9C). There was a paucity of eosinophils in this case (case#1). Tubercular etiology was excluded

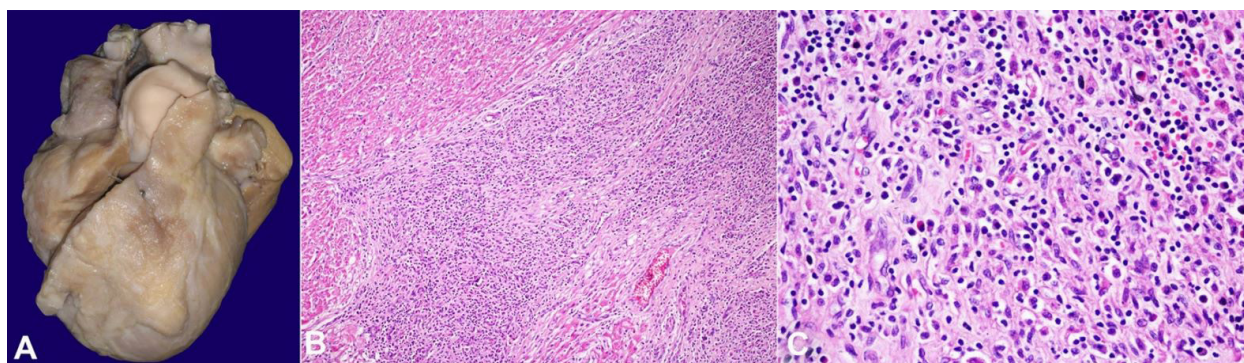


**Figure 7.** Gross view of the heart showing prominent nodular elevation on the anterior surface of right ventricle and right border; **B** and **C** Photomicrographs of the heart – **A** and **B** – depicting infiltration of ventricular wall by LC (H&E, B x200, C x400).

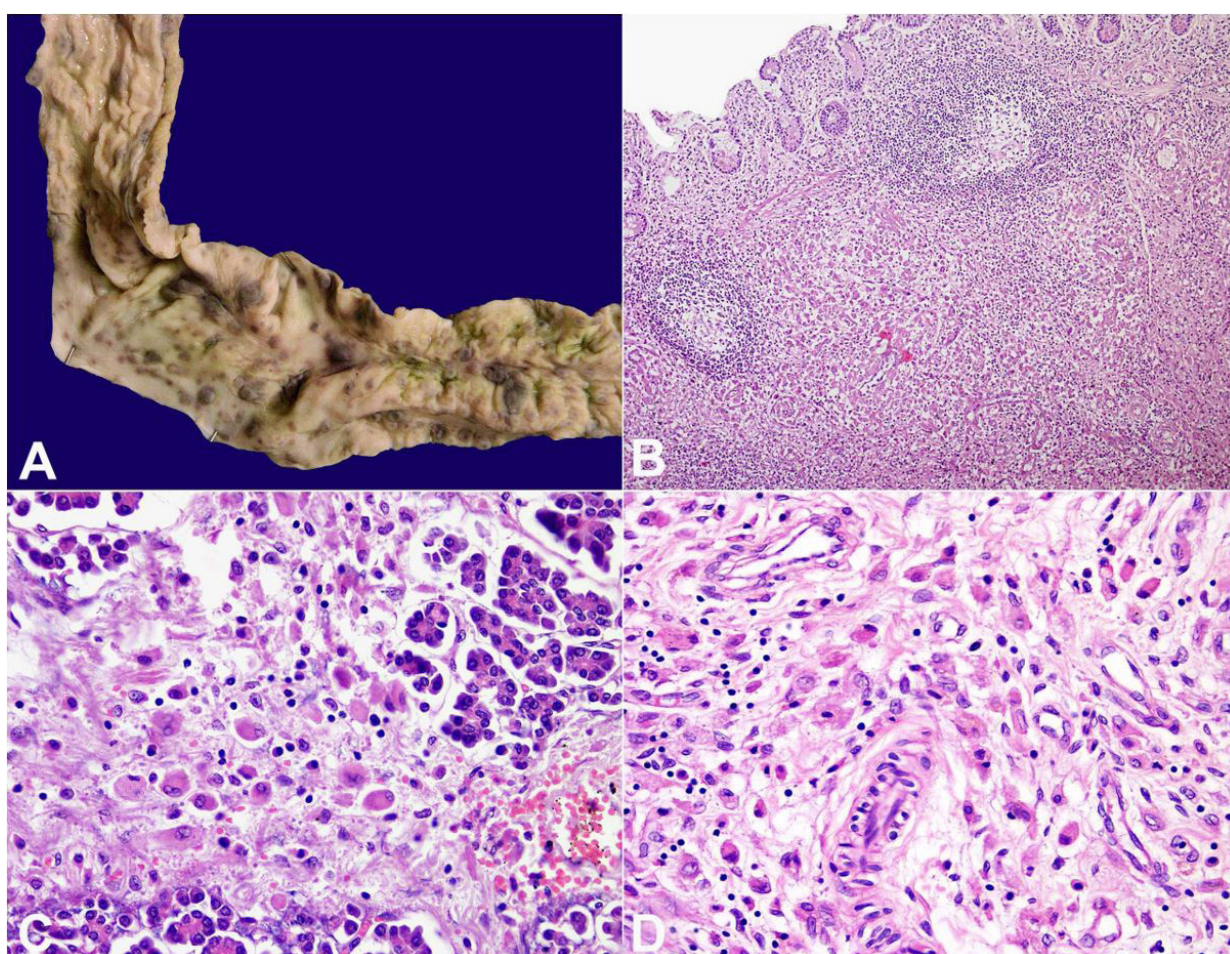


**Figure 8.** **A** – Gross view of the small intestine showing hemorrhagic ulcers; **B** – LC infiltrate expanding the lamina propria (H&E x200); **C** – Infiltrate within the pancreas (H&E x400); **D** – Infiltrate within the thymus (H&E, x400).

by performing polymerase chain reaction (PCR) for tubercular bacilli. Secondary hemophagocytosis was seen in 2 cases (case#1 and case#6).

None of the subjects showed any superadded fungal (negative PAS stain) or tubercular infection

(negative Ziehl-Neelsen stain) except for a single case with *Candida* ulcers in the esophagus (case#1).

### *Mutational Analysis*

RQ-PCR was performed in all six cases in duplicate. Positive control Ct (threshold cycle) values ranged

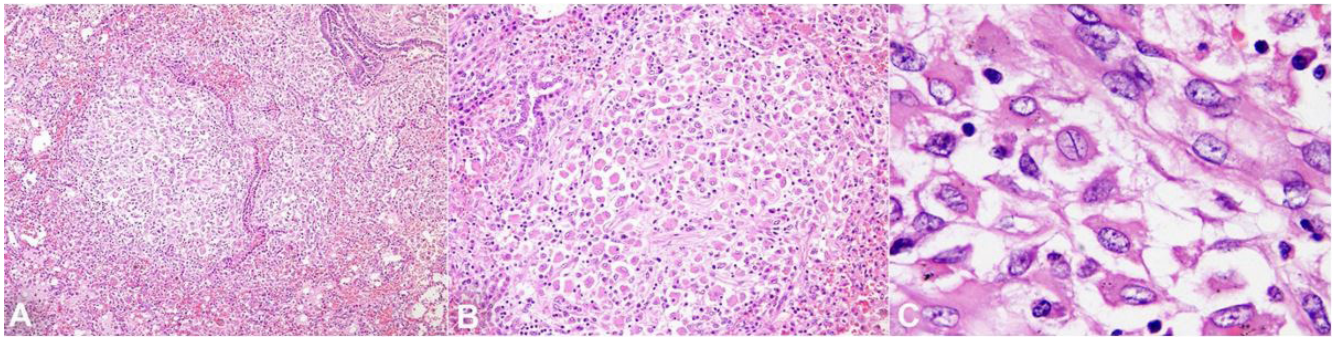


**Figure 9.** Photomicrographs of the lung showing: **A** – LCH granulomas mimicking tuberculosis (H&E x200); **B** – High magnification showing the cellular composition of the infiltrate chiefly composed of LC cells and lymphomononuclear cells (H&E x400); **C** – Photomicrograph in oil immersion field depicting the characteristic grooved nuclei of LC cells (H&E x1000).

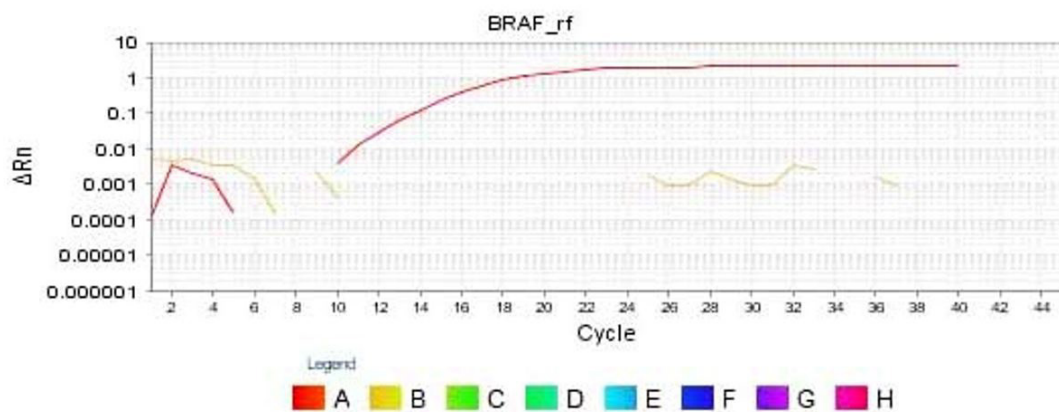


**Figure 10.** RT-PCR result showing BRAF V600E amplification in the control (Red) while the test (yellow) does not show any amplification in any of our cases.

from 22-24.0 with a mean of 23.0. None of the cases showed amplification. Sanger sequencing of the amplified and purified PCR products did not reveal any mutation in the BRAF gene including the hotspot region of BRAF600, as well (Figure 10)

## DISCUSSION

Langerhans cell histiocytosis, a disorder of antigen-presenting cells, the Langerhans-type cells, is the commonest disorder of the mononuclear phagocytic system.<sup>1</sup> The neoplastic cells share immunophenotypic and ultrastructural similarities with Langerhans cells of the epidermis. Due to this resemblance, it was earlier hypothesized that the disease originated from epidermal Langerhans cells; however, lately, the gene profiling studies have indicated their origin from marrow-derived immature myeloid dendritic cells.<sup>13</sup> LCH has a broad spectrum of

clinical manifestations and outcome. Some cases are self-limited, whereas others involve multiple organs and present a high rate of mortality. The etiology remains unknown. The benign morphology of its proliferating cells and its characteristic inflammatory infiltrates, earlier suggested that LCH may be an inflammatory disorder,<sup>14</sup> and dysregulated expression of inflammatory cytokines, such as interleukin-17A, has been reported.<sup>15</sup> Subsequent research provided strong evidence for its neoplastic nature and proved the clonal nature of pathologic LCs.<sup>16,17</sup>

Autopsy studies on LCH are limited to a few case reports.<sup>9,10,18</sup> The findings of this index study highlight interesting aspects of organ infiltration and pattern of infiltration. While hepatomegaly is a common feature of LCH, actual infiltration of the liver is rare, as reported in the literature.<sup>19</sup> However, liver infiltration was noted in all the cases in our study, and was restricted to the presence of LC within the sinusoids

and portal triads. A single case featured an unusual pattern of infiltration in the liver with lesions centered mainly in the periductal location with infiltration and injury to the bile ducts. The involvement of the lymph nodes paralleled that of the liver with infiltration found in all the cases, followed by lungs and spleen. The pulmonary infiltration in systemic LCH has been recently and extensively studied by Kambouchner M et al.,<sup>11</sup> and ranged from nodular pattern with cavitation to cysts, fibrotic scars, or a peribronchiolar distribution of the lesions. Cervical lymph nodes are most commonly involved as compared to other lymph nodes.<sup>20</sup> Histologically, 3 main architectural patterns of LCH in lymph nodes have been described with subtotal effacement of nodal architecture being the commonest.<sup>20</sup> As our cases comprised of autopsy cases with the multi-systemic disease, total effacement of the architecture was the commonest.

Other rare sites of infiltration encountered in this series included the pancreas, GIT, heart, testes, thymus, and choroid plexus. The involvement of GIT and pancreas has been seldom reported in the literature.<sup>9,21</sup> Both, small and large intestine, is involved in equal proportion,<sup>21-23</sup> and the majority occurs in children mostly associated with severe systemic disease. In the present series, one of the cases showed numerous punched out ulcers involving the terminal ileum and whole of the large intestine with extensive infiltrate of LC within the lamina propria. The pancreatic infiltration, in our series, was dominated by inter and intra-lobular fibrosis, ductal dilation, and destruction of acini in three cases, while in a single case, the infiltration was focal. The testis is a very unusual site for infiltration by LC such that it has never been mentioned in the literature. Infiltration of the heart in a single case was very peculiar, seen as nodular masses distorting the pericardial surface and completely replacing the left ventricular and right ventricular wall. This case also showed significant biventricular hypertrophy with grade-II pulmonary arterial hypertension. Heart valves are another common site which is infiltrated; however, we did not observe it in our cohort, especially in the case with the nodular pattern of heart infiltration. Within the central nervous system, the pituitary gland involvement has been reported to be the commonest.<sup>24</sup> We could not substantiate the same in our cases, as consent for brain autopsy could be obtained in a single case, which interestingly revealed infiltration within

the choroid plexus. We did not find much proof to the earlier belief that older lesions tend to contain fewer LCH cells,<sup>25</sup> as in most of our cases, regardless of the age groups, numerous LC within sites of organ infiltration were found. An interesting and novel histological feature observed in two cases was the presence of lymphovascular emboli composed of LC and other inflammatory cells enmeshed in fibrin within the subcapsular sinus of the lymph node.

Clinical presentation and symptoms are varied, ranging from single to multiple organ manifestations. In multisystem LCH, nearly all organs are involved. Pulmonary involvement needs special mention as pulmonary LCH in adults may present as an isolated disease with bilateral nodular infiltrates with the presence of both polyclonal and clonal population of LCs. Thereby, pulmonary LCH is regarded as a distinct entity compared to the childhood LCH.<sup>26</sup> The cause of death in all cases, in this cohort, was both due to an infiltrative disease (n=6/6) and also due to pulmonary involvement resulting in bacterial bronchopneumonia, pulmonary hemorrhage and diffuse alveolar damage. Apart from candida ulcers and early candida abscess in one case, none of the cases had any evidence of fungal/ bacterial or mycobacterial etiology for bronchopneumonia.

A major breakthrough in the pathogenesis of LCH was the identification of recurrent *BRAF V600E* point mutations in approximately 60% of LCH lesions.<sup>6</sup> Currently, the World Health Organization has officially classified the entity as a hematolymphoid tumor. Badalian-Very et al.,<sup>6</sup> detected this mutation in 57% of their cases. Subsequently other series indicate that 38-60% of LCH cases harbor this mutation.<sup>6,7,27</sup> *BRAF V600E* mutations lead to the constitutive activation of the RAS/RAF/MEK/ERK pathway, and ERK activation is the universal endpoint from the various pathological activation occurring upstream. Therefore, LCH is now regarded as neoplastic disease. Furthermore, their findings also indicated the existence of other mutations or translocations, which can result in MAP kinase pathway activation. Next-generation sequencing of LCH lesions subsequently has identified mutations in *MAP2K1*,<sup>28</sup> which occur in 50% of *BRAF* wild-type cases, and mutations in *ARAF*,<sup>29</sup> in sporadic cases. Mutations in *MAP2K1*, that encodes for the dual-specificity kinase MEK1 protein in the MAP kinase pathway were subsequently identified

in 27.5% of LCH cases. *BRAF V600E* and *MAP2K1* mutations were found to be mutually exclusive.<sup>30</sup> None of the cases in our series contained *BRAF V600E* mutation. Recently, this mutation has been proposed to be associated with the most aggressive forms of LCH.<sup>5,12,31</sup> Our finding is surprising, as all our cases had multisystemic involvement with a fatal outcome. However, it has also been reported that Asian patients with LCH tend to show a lower rate of *BRAF V600E* mutation with a frequency ranging from 20-24% in different studies.<sup>32</sup> In a recently published ten-year retrospective data from our group on confirmed LCH cases (2007-2017), we had analyzed 31 formalin-fixed paraffin-embedded biopsy blocks/ cytology Cytoscrabe slides for *BRAF V600E* mutation by both RQ-PCR and Sanger sequencing. Of these, 6/31 (19%) revealed *BRAF V600E* mutation, and all six had multisystem risk organ disease. However, in overall 31 cases, 15 (48%) had multisystem LCH, and 9 out of these were negative for *BRAF V600E* (*unpublished data*). The reason for the absence of *BRAF V600E* might be the presence of other mutations, including *MAP2K1* in our present cohort of six autopsy cases, which needs to be looked into larger prospective studies. In addition, the literature highlights the presence of many other mutations in LCH cases, and these non-recurrent mutations include those in genes like *ARAF*,<sup>29</sup> *ERBB3*,<sup>7</sup> *PI3KCA*,<sup>33</sup> and *MAP3K1*<sup>28</sup> with frequency ranging from 17% to 27.5%<sup>7,30</sup> in cases with wild type *BRAF*. Another reason for the absence of mutation might be that we did not use low allele detection methods like digital droplet PCR or deep sequencing by next-generation sequencing technique, which have a very high sensitivity to pick somatic mutations with low frequency. Detecting these mutations (*BRAF V600E* and *MAP2K1*) has both prognostic and therapeutic relevance.<sup>34</sup> Vemurafenib, an inhibitor of *BRAF*, has already been shown to be effective in the treatment of melanoma and hairy cell leukemia that harbor *BRAF* mutations.

In conclusion, this autopsy series illustrates the different patterns, extent, and sites of organ infiltration in LCH. Some rare sites, which hitherto have not been documented in the literature, have been highlighted. This is particularly important as such data gives important clues for early diagnosis and timely intervention. Apart from testing for *BRAF V600E* mutations, other mutations resulting in activation of the MAP kinase pathway should also be assessed.

### Key Messages:

- Langerhans cell histiocytosis has a variable clinical presentation;
- Apart from its classic organ infiltration described in reticuloendothelial system, skin and bones; it infrequently may infiltrate heart, thymus, choroid plexus and testis;
- Pulmonary infiltration is seen as nodular bronchiolocentric infiltration of LCH cells;
- Lymphovascular emboli of LCH cells, extremely uncommon, can also occur;
- Frequency of activating *BRAF V600E* mutation is variable, with some regions reporting a low frequency as was also noted in this study.

### REFERENCES

1. Haupt R, Minkov M, Astigarraga I, et al. Langerhans cell histiocytosis (LCH): guidelines for diagnosis, clinical work-up, and treatment for patients till the age of 18 years. *Pediatr Blood Cancer*. 2013;60(2):175-84. <http://dx.doi.org/10.1002/psc.24367>. PMID:23109216.
2. Gadner H, Heitger A, Grois N, Gatterer-Menz I, Ladisch S. Treatment strategy for disseminated Langerhans cell histiocytosis. *Med Pediatr Oncol*. 1994;23(2):72-80. <http://dx.doi.org/10.1002/mpo.2950230203>. PMID:8202045.
3. Lau L, Krafchik B, Trebo M, Weitzman S. Cutaneous Langerhans cell histiocytosis in children under one year. *Pediatr Blood Cancer*. 2006;46(1):66-71. <http://dx.doi.org/10.1002/psc.20479>. PMID:16261594.
4. Suri HS, Yi ES, Nowakowski GS, et al. Pulmonary Langerhans cell histiocytosis. *Orphanet J Rare Dis*. 2012;19:7-16. PMID:22429393.
5. Heritier S, Emile JF, Barkaoui MA, et al. *BRAF* mutation correlates with high-risk Langerhans cell Histiocytosis and increased resistance to first line therapy. *J Clin Oncol*. 2016;34(25):3023-30. <http://dx.doi.org/10.1200/JCO.2015.65.9508>. PMID:27382093.
6. Badalian-Very G, Vergilio JA, Degar BA, et al. Recurrent *BRAF* mutations in Langerhans cell histiocytosis. *Blood*. 2010;116(11):1919-23. <http://dx.doi.org/10.1182/blood-2010-04-279083>. PMID:20519626.
7. Chakraborty R, Hampton OA, Shen X, et al. Mutually exclusive recurrent somatic mutations in *MAP2K1* and *BRAF* support a central role for ERK activation in LCH pathogenesis. *Blood*. 2014;124(19):3007-15. <http://dx.doi.org/10.1182/blood-2014-05-577825>. PMID:25202140.
8. Berres ML, Lim KP, Peters T, et al. *BRAF-V600E* expression in precursor versus differentiated dendritic cells defines clinically distinct LCH risk groups. *J Exp*

- Med. 2014;211(4):669-83. <http://dx.doi.org/10.1084/jem.20130977>. PMID:24638167.
9. Goyal R, Das A, Nijhawan R, Bansal D, Marwaha RK. Langerhans cell histiocytosis infiltration into pancreas and kidney. *Pediatr Blood Cancer*. 2007;49(5):748-50. <http://dx.doi.org/10.1002/pbc.20746>. PMID:16411199.
  10. Gupta K, Bansal A, Mathew JL, et al. Pulmonary nodules with central cavitation in a young child. *J Pediatr Hematol Oncol*. 2013;35(4):307, 331-3. <http://dx.doi.org/10.1097/MPH.0b013e31826ef939>. PMID:23007420.
  11. Kambouchner M, Emile JF, Copin MC, et al. Childhood pulmonary Langerhans cell histiocytosis: a comprehensive clinical-histopathological and BRAFV600E mutation study from the French national cohort. *Hum Pathol*. 2019;89:51-61. <http://dx.doi.org/10.1016/j.humpath.2019.04.005>. PMID:31054893.
  12. Liu X, Zhang Y, Zhou CX. High prevalence of BRAF V600E mutations in langerhans cell histiocytosis of head and neck in chinese patients. *Int J Surg Pathol*. 2019;1066896919855774(8):1066896919855774. <http://dx.doi.org/10.1177/1066896919855774>. PMID:31203679.
  13. Collin M, Bigley V, McClain KL, Allen CE. Cell(s) of origin of langerhans cell histiocytosis. *Hematol Oncol Clin North Am*. 2015;29(5):825-38. <http://dx.doi.org/10.1016/j.hoc.2015.06.003>. PMID:26461145.
  14. Broadbent V, Davies EG, Heaf D, et al. Spontaneous remission of multi-system histiocytosis X. *Lancet*. 1984;1(8371):253-25. [http://dx.doi.org/10.1016/S0140-6736\(84\)90127-2](http://dx.doi.org/10.1016/S0140-6736(84)90127-2). PMID:6142997.
  15. Coury F, Annels N, Rivollier A, et al. Langerhans cell histiocytosis reveals a new IL-17A-dependent pathway of dendritic cell fusion. *Nat Med*. 2008;14(1):81-7. <http://dx.doi.org/10.1038/nm1694>. PMID:18157139.
  16. Willman CL, Busque L, Griffith BB, et al. Langerhans'-cell histiocytosis (histiocytosis X): a clonal proliferative disease. *N Engl J Med*. 1994;331(3):154-60. <http://dx.doi.org/10.1056/NEJM199407213310303>. PMID:8008029.
  17. Yu RC, Chu AC, Chu C, Buluwela L. Clonal proliferation of Langerhans cells in Langerhans cell histiocytosis. *Lancet*. 1994;343(8900):767-8. [http://dx.doi.org/10.1016/S0140-6736\(94\)91842-2](http://dx.doi.org/10.1016/S0140-6736(94)91842-2). PMID:7510816.
  18. Trotz M, Weber MA, Jacques TS, Malone M, Sebire NJ. Disseminated langerhans cell histiocytosis-related sudden unexpected death in infancy. *Fetal Pediatr Pathol*. 2009;28(1):39-44. <http://dx.doi.org/10.1080/15513810802548099>. PMID:19116814.
  19. Favara BE. Histopathology of the liver in histiocytosis syndromes. *Pediatr Pathol Lab Med*. 1996;16(3):413-33. PMID:9025843.
  20. Edelweiss M, Medeiros LJ, Suster S, Moran CA. Lymph node involvement by Langerhans cell histiocytosis: a clinicopathological and immunohistochemical study of 20 cases. *Hum Pathol*. 2007;38(10):1463-9. <http://dx.doi.org/10.1016/j.humpath.2007.03.015>. PMID:17669469.
  21. The French Langerhans' Cell Histiocytosis Study Group. A multicentre retrospective survey of Langerhans' cell histiocytosis: 348 cases observed between 1983 and 1993. *Arch Dis Child*. 1996;75(1):17-24. <http://dx.doi.org/10.1136/adc.75.1.17>. PMID:8813865.
  22. Yadav SP, Kharya G, Mohan N, et al. Langerhans cell histiocytosis with digestive tract involvement. *Pediatr Blood Cancer*. 2010;55(4):748-53. <http://dx.doi.org/10.1002/pbc.22663>. PMID:20535829.
  23. Behdad A, Owens SR. Langerhans cell histiocytosis involving the gastrointestinal tract. *Arch Pathol Lab Med*. 2014;138(10):1350-2. <http://dx.doi.org/10.5858/arpa.2014-0290-CC>. PMID:25268199.
  24. Grois N, Fahrner B, Arceci RJ, et al. Central nervous system disease in Langerhans cell histiocytosis. *J Pediatr*. 2010;156(6):873-881.e1. <http://dx.doi.org/10.1016/j.jpeds.2010.03.001>. PMID:20434166.
  25. Yu RC, Attra A, Quinn CM, Krausz T, Chu AC. Multisystem Langerhans cell histiocytosis with pancreatic involvement. *Gut*. 1993;34(4):570-2. <http://dx.doi.org/10.1136/gut.34.4.570>. PMID:8491411.
  26. Allen TC. Pulmonary Langerhans cell histiocytosis and other pulmonary histiocytic diseases: a review. *Arch Pathol Lab Med*. 2008;132(7):1171-81. PMID:18605769.
  27. Sahn F, Capper D, Preusser M, et al. BRAFV600E mutant protein is expressed in cells of variable maturation in Langerhans cell histiocytosis. *Blood*. 2012;120(12):e28-34. <http://dx.doi.org/10.1182/blood-2012-06-429597>. PMID:22859608.
  28. Nelson DS, Halteren A, Quispel WT, et al. MAP2K1 and MAP3K1 mutations in Langerhans cell histiocytosis. *Genes Chromosomes Cancer*. 2015;54(6):361-8. <http://dx.doi.org/10.1002/gcc.22247>. PMID:25899310.
  29. Nelson DS, Quispel W, Badalian-Very G, et al. Somatic activating ARAF mutations in Langerhans cell histiocytosis. *Blood*. 2014;123(20):3152-5. <http://dx.doi.org/10.1182/blood-2013-06-511139>. PMID:24652991.
  30. Brown NA, Furtado LV, Betz BL, et al. High prevalence of somatic MAP2K1 mutations in BRAF V600E-negative Langerhans cell histiocytosis. *Blood*. 2014;124(10):1655-8. <http://dx.doi.org/10.1182/blood-2014-05-577361>. PMID:24982505.
  31. Mehes G, Irsai G, Bedekovics J, et al. Activating BRAF V600E mutation in aggressive pediatric Langerhans cell histiocytosis: demonstration by allele-specific PCR/direct sequencing and immunohistochemistry. *Am J Surg Pathol*. 2014;38(12):1644-8. <http://dx.doi.org/10.1097/PAS.0000000000000304>. PMID:25118810.

32. Sasaki Y, Guo Y, Arakawa F, et al. Analysis of the BRAFV600E mutation in 19 cases of Langerhans cell histiocytosis in Japan. *Hematol Oncol*. 2017;35(3):329-34. <http://dx.doi.org/10.1002/hon.2293>. PMID:27041734.
33. He'ritier S, Saffroy R, Radosevic-Robin N, et al. Common cancer-associated PIK3CA activating mutations rarely occur in Langerhans cell histiocytosis. *Blood*. 2015;125(15):2448-9. <http://dx.doi.org/10.1182/blood-2015-01-625491>. PMID:25858893.
34. Abla O, Weitzman S. Treatment of Langerhans cell histiocytosis: role of BRAF/MAPK inhibition. *Hematology (Am Soc Hematol Educ Program)*. 2015;2015(1):565-70. <http://dx.doi.org/10.1182/asheducation.V2015.1.565.3919688>. PMID:26637773.

**Authors' contributions:** Kapatia G assisted in pathology analysis, critically reviewed the literature, and contributed to preparing the manuscript. Gupta K critically reviewed the literature, performed the pathology analysis and prepared the manuscript. Bansal D and Jain R actively participated in antemortem clinical management of the patients. Bhatia P and Singh M critically reviewed the literature and provided the molecular diagnosis. All authors proofread the final manuscript and approved it to publication.

The family members of the patients signed the consent declaration. The manuscript's conception has been approved by the Research Ethical Committee of the institution.

**Conflict of interest:** None

**Financial support:** None

**Submitted on:** December 26<sup>th</sup>, 2019

**Accepted on:** January 30<sup>th</sup>, 2020

### Correspondence

Kirti Gupta

Department of Histopathology - Postgraduate Institute of Medical Education and Research (PGIMER)  
Sector 12. Chandigarh – India

Pin code: 160012

Phone: +91 (172) 2755105 / Fax: +91 (172) 2744401

kirtigupta10@yahoo.co.in